Regional Alveolar Pressure during Periodic Flow

Dual Manifestations of Gas Inertia

Julian L. Allen, Ivan D. Frantz III, and Jeffrey J. Fredberg
Department of Pediatrics, Harvard Medical School, Boston, Massachusetts 02115; and
The Biomechanics Institute, Boston, Massachusetts 02215

Abstract

We measured pressure excursions at the airway opening and at the alveoli (P_A) as well as measured the regional distribution of P_A during forced oscillations of six excised dog lungs while frequency (f [2–32 Hz]), tidal volume (V_T [5–80 ml]), and mean transpulmonary pressure (P_L [25, 10, and 6 cm H_2O]) were varied. P_A's were measured in four alveolar capsules glued to the pleura of different lobes. The apex-to-base ratio of P_A's was used as an index of the distribution of dynamic lung distension. At low f, there was slight preferential distension of the lung base which was independent of V_T, but at higher f, preferential distension of the lung apex was found when V_T's were small, whereas preferential distension of the lung base was found when V_T's approached or exceeded dead space. These V_T-related changes in distribution at high frequencies seem to depend upon the branching geometry of the central airways and the relative importance of convective momentum flux vs. unsteady inertia of gas residing therein, which, in this study, we showed to be proportional to the ratio V_T/V_D*, where V_D* is an index of dead space. Furthermore, they imply substantial alteration in the distribution of ventilation during high frequency ventilation as f, V_T, and P_L vary. The data also indicate that alveolar and airway opening pressure costs per unit flow delivered at the airway opening exhibit weakly nonlinear behavior and that resonant amplification of P_A's, which has been described previously for the case of very small V_T's, persists but is damped as V_T's approach dead space values.

Introduction

When pleural pressure is uniform, as in a dog whose chest has been opened, or in its excised lung, tidal volume (V_T)[1] is distributed in accordance with the impedance of parallel pathways, with lower impedance pathways receiving a larger share and smaller time-constant pathways receiving their shares earlier (1). This impedance-controlled distribution implies that regional V_T and interregional asynchrony of lung filling are controlled by the distribution of compliances at very low frequencies (2, 3), by the distribution of resistance-compliance time constants at somewhat higher frequencies (1), by the distribution of resistance/inertance time constants above resonant frequency, and by the distribution of inertances at still higher frequencies (4–6). By definition, these ideas are cast within the framework of linear mechanical descriptions of both lung tissue deformations and airway gas flows.

Some evidence suggests that the distribution of V_T's may depart from the impedance-controlled distributions when inspiratory flow rates become large. In such circumstances, regional lung distension might be controlled, at least in part, by the distribution of nonlinear (i.e., amplitude-dependent) features, such as the pressure-volume elastic characteristic of lung parenchyma, flow-dependent changes in airways resistances, convective momentum flux per unit area (ρu^2)—also known as dynamic head—and by associated fluidic factors, such as airway branching angles, distal airway pressures, and Reynolds numbers. Flow-dependent changes in flow distribution have been observed in in vitro airway models (7–11) and in humans (12–15). Computational models that predict flow-dependent alterations in the distribution of inspired gas have incorporated nonlinearities of flow resistance and tissue elasticity, but as yet have not dealt with nonlinear manifestations of fluid inertia (16, 17).

In the case of high frequency ventilation (HFV), inspiratory flow rates span the range including and exceeding those encountered under ordinary physiological conditions. Venegas et al. (18) have used washouts of radioactive trace gases during HFV to demonstrate that the healthy canine lung in situ clears relatively uniformly when V_T's are small compared with dead space, but that basal regions clear more rapidly when V_T's are larger. Similarly, Brusasco et al. (19) and Schmid et al. (20) have shown that regional clearance rates are relatively uniform, but vary with V_T and frequency (f) among apical, basal-dependent, and basal-nondependent regions. The mechanical basis for these regional nonhomogeneities of gas exchange is unknown.

This paper deals with the following: (*a*) the regional distribution of lung distension and the mechanical factors that control it when frequencies are as high as 32 Hz and V_T's span dead space values; and (*b*) the pressure costs of distending lung tissues under such circumstances. In both regards, linear descriptions of the oscillatory mechanics of the lung, as embodied in impedance models, might be expected to be inadequate. To address these questions, we employed the alveolar capsule method in excised canine lungs to obtain direct measurements of regional alveolar pressures (21). Because regional alveolar pressure is closely coupled to regional lung

This study was presented in part at the 68th Annual Meeting of the Federation of American Societies for Experimental Biology, St. Louis, MO, 3 April 1984, and published in abstract form in 1984. *Fed. Proc.* 43:508.

Address correspondence to Dr. Allen, Pulmonary Division, The Children's Hospital, 300 Longwood Ave., Boston, MA 02115. Dr. Allen is a Parker B. Francis fellow of the Puritan-Bennett Foundation.

Received for publication 3 December 1984 and in revised form 5 April 1985.

1. *Abbreviations used in this paper:* C_L, lung compliance; f, frequency; HFV, high frequency ventilation; I_{ab}, apex-to-base ratio of alveolar pressure excursions; P_A, pressure excursion at the alveoli; P_{ao}, pressure excursion at the airway opening; P_{cm}, pressure associated with convective momentum of gas; P_L, transpulmonary distending pressure; P_{ua}, unsteady inertial pressure required for the temporal acceleration of airways gas over the course of a cycle; $\dot{V}_{ao}$, peak-to-peak flow excursion; V_T, tidal volume.

J. Clin. Invest.

0021-9738/85/08/0620/10 $1.00
Volume 76, August 1985, 620–629

volume through the pressure-volume relation of lung tissue, alveolar pressure may be regarded as a crude index of regional lung volume, as if each alveolar capsule were a regional volume plethysmograph, so to speak. Our findings indicate that at low frequencies, distension of the lung base is favored slightly independent of V_T, but at higher frequencies distension of the lung apex is favored when V_T's are small, whereas distension of the lung base is favored when V_T's approach or exceed dead space. These V_T–related changes in distribution at high frequencies seem to depend upon the branching geometry of the central airways and the relative importance of convective momentum flux and unsteady inertia of gas residing therein. Our data also show that resonant amplification of alveolar pressure excursions, which has been described for the case of very small V_T's (21, 22), persists, but is damped as tidal volumes approach dead space values.

Methods

To characterize the mechanical behavior of the lung under a wide variety of oscillatory conditions, we focused these studies upon peak-to-peak pressure excursions, both at the alveoli and the airway opening. The rationale in choosing these descriptors was to obtain crude bounds on the distending pressures to which airway walls and lung tissues were exposed, without regard to the time course through which these extremes were achieved. In doing so, data could be expressed simply and compactly, but all information regarding waveform shapes, harmonic distortions, temporal relationships between pressure and flow (and implicitly lung resistance), and asynchrony of regional lung filling was lost. To the degree that any of these measures is a more sensitive index of nonlinear behavior vis-a-vis peak-to-peak excursions, evidence of nonlinear behavior would be less evident in our data.

Animal preparation. The excised lungs of six adult dogs (mean weight 11.7 kg) were studied. The dogs were pretreated with atropine (1 mg s.c.) and one-half hour later were anesthetized with pentobarbital (25 mg/kg i.v.). To minimize gas trapping, we administered 1 mg/kg of atropine, followed by 0.08 mg/kg of phentolamine (regitine HCL) one-half hour later (Lehr, J., personal communication). The dogs were then given 10,000 U of heparin sulfate and exsanguinated through a femoral artery catheter. The lungs were collapsed by a substernal blunt dissection into the pleural space. After an in situ pressure-volume curve was obtained, the lungs, trachea up to the glottis, and heart were removed en bloc. The heart was then separated from the rest and the lungs were degassed. The mean vital capacity, defined as the volume difference between 0 and 25 cm H_2O distending pressure, was 829±126 (SD) ml.

Apparatus. Periodic flow was generated by a piston pump, with V_T varied by positioning the piston shaft along an eccentric cam (Fig. 1). Brusasco et al. (23) have shown that during HFV the gas volume delivered to the lung may not necessarily equal the stroke volume of the piston pump, particularly near the resonant frequency of the HFV circuit. So that we could use piston pump displacement as a reliable index of volume delivered to the lung, the pump was designed to minimize the distance between the piston face and trachea, and to keep the ports between the pump and trachea relatively large in cross-section. In this way, we minimized inertial and resistive pressures generated within the pump chamber, and thereby the potential for gas compression. To validate that pump volumetric displacement was a good approximation of volume delivered to the lung for our particular experimental configuration, the pump outlet was attached to tubes of 7.9 mm internal diameter and of 15 and 27.5 cm length terminated into a pressure plethysmograph. Plethysmographically determined V_T's matched pump displacements to within 5% throughout most of the frequencies and V_T's studied. Studying the longest tube, we found that when both the frequency and V_T were simultaneously greatest (32 Hz, 80 ml) driving pressures within the piston chamber approached 300 cm H_2O, and the delivered V_T's were 20% less than pump volumetric

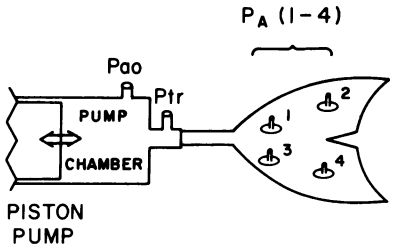

Figure 1. Piston pump generates oscillatory flow into the lung, with alveolar capsules attached. Distending pressure is measured at the pump chamber by a water manometer. Abbreviations as in text.

displacement. In the animal studies, however, peak-to-peak pressure excursions in the chamber never exceeded 50 cm H_2O, and thus errors in V_T estimation are expected to be substantially <20% and more typically 5% or less.

A mechanical pressure control system, the Emerson popoff valve (J. H. Emerson Co., Cambridge, MA), kept the lung inflated to the desired mean transpulmonary distending pressure (P_L) as monitored at the piston pump chamber by a water manometer. Both the manometer and pressure control system were connected to the pump chamber through high impedance tubing. Because chamber cross-section was large (5.7 cm i.d.), linear velocities and the dynamic head were small (<0.2 cm H_2O), and the mean side hole pressure in the chamber relative to atmosphere represented true transpulmonary pressure.

We used a capsule technique that has been described and validated previously (21) for sampling alveolar pressures. In brief, the capsule consisted of a flat based plastic chamber. The flat surface of each capsule was glued to the lung surface with a cyanoacrylate base glue (Krazy Glue; Krazy Glue, Inc., Kiasca, IL) at four locations: the left and right apical lobes and the left and right diaphragmatic lobes. Four to six holes 2 mm deep were punctured in the pleural surface, creating continuity between alveolar gas and capsule gas. Piezoresistive pressure transducers (model 8510-2; Endevco Corp., San Juan Capistrano, CA) with flat frequency response to 40,000 Hz, and linear response to pressures of ±140 cm H_2O, were securely fitted into the capsules via a short length (<1 cm) of stiff tubing. Each pressure signal was amplified by an amplifier (model AM502; Tektronix, Inc., Beaverton, OR) and band-pass filtered from 2 to 80 Hz.

Protocol. Primary quantities measured were oscillatory f, V_T, and peak-to-peak pressure excursions at the airway opening (P_{ao}), at the trachea (P_{tr}), and in the four peripheral alveolar sites (P_A) (Fig. 1). V_T's studied were 5, 10, 20, 40, and 80 ml. The oscillatory f was swept from 2 to 32 Hz, with the flows closely approximating a sinusoid. At each V_T, experiments were repeated on the descending limb of the pressure-volume curve after deflation from a P_L of 30 cm H_2O to 25, 10, or 6 cm H_2O as measured at the pump chamber relative to atmosphere. In one half of the animals studied, V_T's were then systematically increased from 5 to 80 ml. In the other half, they were decreased from 80 to 5 ml.

The peak-to-peak pressure excursions were displayed on a storage oscilloscope with dynamic pressure signals from each transducer on the y axis, as a function of oscillatory frequency from 0 to 32 Hz on the x axis. All pressure excursions reported refer to peak-to-peak excursions about the mean distending pressure regardless of waveform shape. The peak-to-peak flow excursion, $\dot{V}_{ao}$, was calculated from the equation $\dot{V}_{ao} = 2\pi f V_T$.

Data analysis. The experiments often involved nonlinear behavior. Even though the flow waveform was almost sinusoidal, pressure signals observed were often quite distorted as a result of nonlinear lung mechanics. In the present study, we restricted our attention to the peak-to-peak amplitude of the pressure excursions rather than their temporal character.

Even in the nonlinear case, several useful normalizations of pressure can be adapted from linear oscillation mechanics. In the normalizations described below, frequency refers to piston pump frequency, and all physical quantities refer to peak-to-peak excursions about the mean, and include any harmonic distortions that might have been engendered by mechanical nonlinearities within the lung. $P_{ao}/\dot{V}_{ao}$ represents the

peak-to-peak pressure response within the pump chamber per unit peak-to-peak flow excursion, which reduces to lung impedance (Z_L) in the case of infinitesimal tidal volumes. $P_A/\dot{V}_{ao}$ represents the alveolar pressure response per unit flow at the airway opening. When airway wall distension and gas compression are small, $\dot{V}_{ao}$ also represents flow through lung tissues. If, further, V_T is infinitesimal, then $P_A/\dot{V}_{ao}$ reduces to lung tissue impedance. In general, however, this is not assumed.

To measure the relative magnitude of alveolar and airway opening pressure excursions, we computed the alveolar pressure ratio, P_A/P_{ao}, by taking the ratio of peak-to-peak alveolar pressure excursions at individual capsules, averaged over all sites, to those at the pump chamber. To assess interregional nonhomogeneity, we computed the relative magnitude of apex-to-base alveolar pressure excursions (I_{ab}), by $(P_{A1} + P_{A3})/(P_{A2} + P_{A4})$, where capsules 1 and 3 were on either apical lobe and capsules 2 and 4 were on either diaphragmatic lobe (Fig. 1). P_A/P_{ao} and I_{ab} were calculated for each dog, and then averaged for all dogs.

Regional nonhomogeneities in tissue properties are not an intrinsic limitation in interpretation of I_{ab}. In the case of quasistatic low frequency small amplitude inflations, all intrapulmonary gas is in hydrostatic equilibrium, and so the capsules must register a homogeneous distribution of alveolar pressure. Thus for quasistatic maneuvers regional nonuniformities of tissue properties lead to nonuniform lung expansion but uniform alveolar pressure (24, 25), and by definition, I_{ab} must be unity. Any subsequent departure of I_{ab} from unity under dynamic circumstances can be interpreted as a frequency-dependent departure in distribution of lung distension in excess of the elastically determined quasistatic nonhomogeneity, which serves as base line. This is seen as a considerable advantage of the alveolar capsule method for the present study, in which the effect of f and V_T in altering the distribution of inspired gas is of interest but the quasistatic distribution is not. Furthermore, while in the excised lung lobar elastic properties do tend to be systematically different, these differences are relatively small and of little consequence here (24, 25). Thus, I_{ab} is taken as a crude index of the relative distension of the lung apex compared with the base.

Results

Peak-to-peak pressure excursions within the pump chamber (P_{ao}) and at the proximal end of the trachea (P_{tr}) were very nearly equal, although tracheal pressure excursions were slightly smaller than chamber pressure excursions when both were >10 cm H_2O peak-to-peak.

P_{ao}, resulting from sweeps at fixed V_T, exhibited a plateau at low frequencies, a rise at higher frequencies, and sometimes exhibited a minimum at intermediate frequencies, particularly at the higher distending pressures (Fig. 2). These pressure excursions increased in almost direct proportion to V_T. At lower frequencies, pressure excursions increased with P_L, but at higher frequencies tended to vary little with P_L. In most circumstances, chamber pressure remained positive with respect to atmosphere throughout the cycle, but chamber pressure became negative with respect to atmosphere during parts of the cycle when frequency and tidal volume were large while P_L was small. At the largest $f \times V_T$ products, we noted expansion of the trachea during inspiration and marked collapse during expiration.

P_A increased with increasing f, but exhibited far less f dependence than did P_{ao} (Fig. 3). These pressure excursions also increased in nearly direct proportion to V_T. Throughout, the f range examined P_A increased with increasing distending pressure.

These data could be collapsed effectively by normalizing pressure by flow delivered at the airway opening, i.e., by expressing them as impedances. Chamber pressure (P_{ao}) per unit flow ($\dot{V}_{ao}$) exhibited the classical behavior of a series inertance-resistance-compliance system (Fig. 4), with a compliance-controlled region at low frequencies (impedance diminishing nearly as $1/f$), a resonant resistance-controlled region at intermediate frequencies (impedance minimum), and an inertially controlled region at higher frequencies (impedance increasing as f). Remarkably, when normalized by $\dot{V}_{ao}$, these data showed relatively slight influence of V_T. With a 16-fold increase of V_T, the qualitative features were unaltered, and the quantitative nature changed comparatively little. At all frequencies and distending pressures studied, V_T changes of 16-fold led to lung impedance changes of less than twofold, and in most cases far less. These changes were not always well ordered with respect to V_T. In addition, the resonant frequency shifted to slightly lower values in the case of the highest V_T studied (80 ml), at P_L of 10 and 25 cm H_2O. With increasing P_L, the compliance decreased with a corresponding shift in resonant frequency. The inertially controlled impedances were relatively insensitive to changes in P_L.

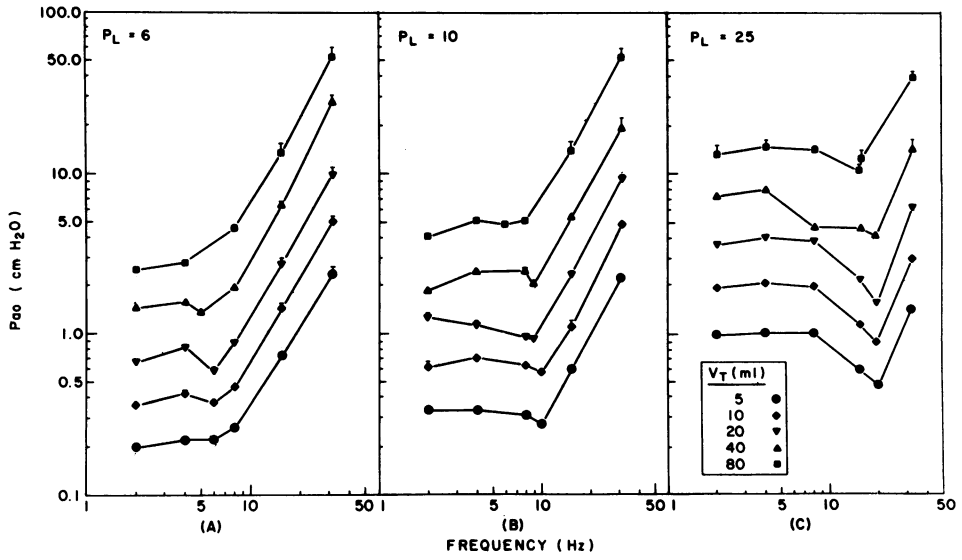

Figure 2. Pressure excursions at the pump chamber (P_{ao})±SEM vs. oscillatory frequency, at differing V_T's and distending pressures (P_L). (*A*) P_L = 6 cm H_2O; (*B*) P_L = 10 cm H_2O; (*C*) P_L = 25 cm H_2O. Where standard error bars are not shown they are smaller than the symbol designating the mean value.

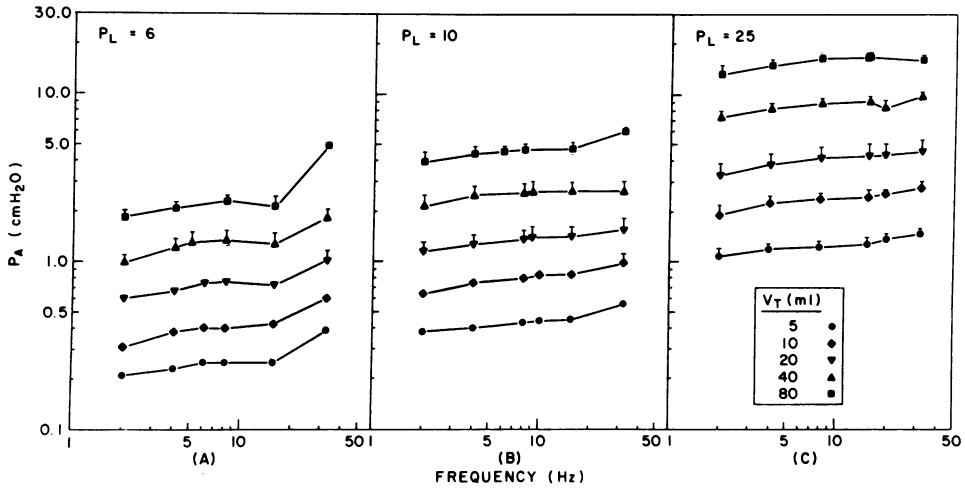

Figure 3. Alveolar pressure excursions (P_A)±SEM, averaged over all capsule sites, vs. oscillatory frequency at differing V_T's and distending pressures. (*A*) P_L = 6 cm H_2O; (*B*) P_L = 10 cm H_2O; (*C*) P_L = 25 cm H_2O. Where standard error bars are not shown, they are smaller than the symbol designating the mean value.

P_A data also could be collapsed effectively by expressing them as P_A per unit flow delivered at the airway opening, $\dot{V}_{ao}$ (Fig. 5). These data revealed elastically controlled behavior for the most part, with pressure per unit flow falling in nearly inverse proportion to frequency. More than in the case of lung impedance, these data exhibited a well ordered but small dependence upon V_T, with 16-fold changes in V_T producing only a twofold change in impedance at P_L of 6 cm H_2O, and far less at larger distending pressures. This dependence upon V_T was inverse, with $P_A/\dot{V}_{ao}$ falling systematically with increasing V_T at nearly every f and mean distending pressure. P_A per unit flow was also strongly dependent on distending pressure, increasing with P_L at any given combination of f and V_T.

Alveolar pressure ratio. For a given V_T and P_L, the ratio of alveolar pressure excursions to those at the airway opening was close to unity at low frequencies, achieved a maximum value near the lung resonant frequency, and fell thereafter to a value less than unity at higher frequencies (Fig. 6). For a given transpulmonary pressure the peak value of the pressure ratio tended to occur at slightly lower frequencies as V_T increased. The peak value also tended to fall with increasing V_T but not in a well-ordered fashion. At a given V_T the peak value increased with increasing transpulmonary pressure.

Interregional differences. Nonhomogeneity of pressure excursions between apical and basilar capsules varied systematically with f, V_T, and P_L (Figs. 7 and 8). At low frequencies and at all transpulmonary pressures, I_{ab} was slightly less than unity and was f and V_T invariant. With increasing distending pressure, this invariance with f and V_T persisted to higher frequencies, and I_{ab} fell closer to unity. As frequencies approached and exceeded lung resonant frequency, as noted from the impedance minima of Fig. 4, I_{ab} tended to fall and then exhibit frequency dependence that varied strongly with V_T, with smaller V_T's favoring increased I_{ab}, and vice versa. Much smaller right- vs. left-sided differences in alveolar pressure were found at any f, V_T, or distending pressure (Fig. 7).

Discussion

The principal finding of this report is that regional lung distension during periodic flow was nonuniform, with distension of the lung base favored increasingly as V_T increased. This represents an important departure from the linear small amplitude case. Even so, P_{ao} and P_A (averaged over all units) per unit flow were remarkably well characterized by classical small amplitude linear mechanics. Also, we found that the amplification of P_A relative to those at P_{ao}, which had been noted previously under conditions of smaller V_T's (21, 22), persisted at higher V_T's.

Limitations of linear descriptions. Peak-to-peak pressure data (Figs. 2 and 3) were normalized effectively by flow at the

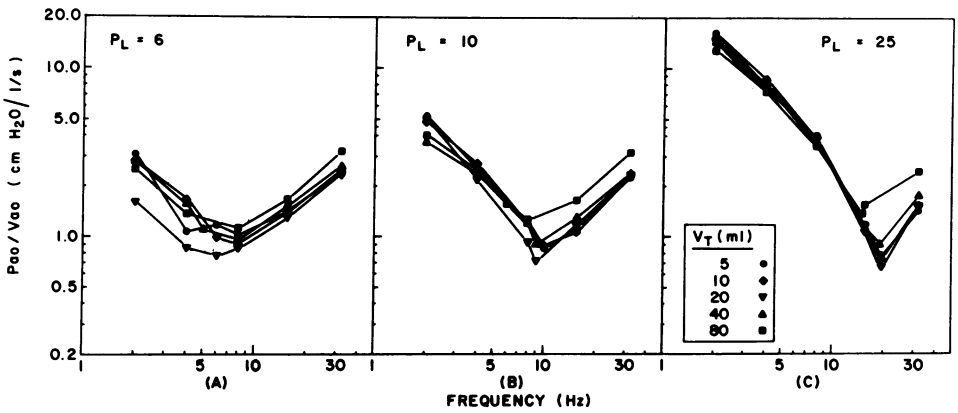

Figure 4. Airway opening pressure excursions per unit flow at the airway opening vs. oscillatory frequency at differing V_T's and distending pressures. (*A*) P_L = 6 cm H_2O; (*B*) P_L = 10 cm H_2O; (*C*) P_L = 25 cm H_2O; l, liter.

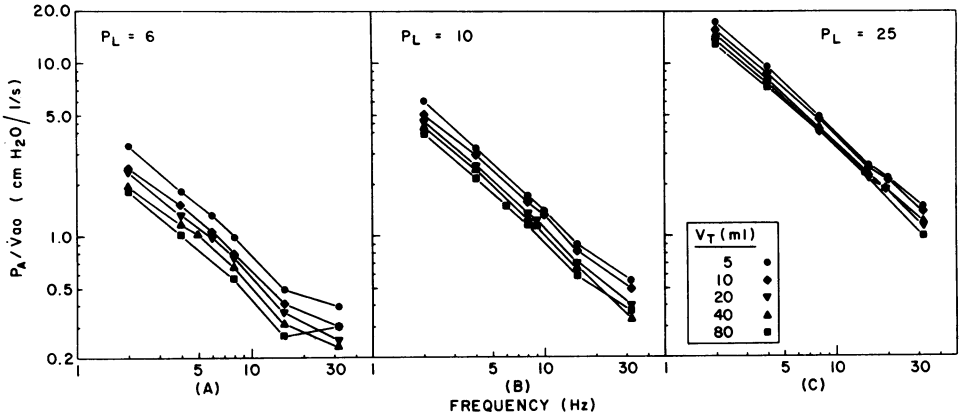

Figure 5. Alveolar pressure excursions per unit flow at the airway opening vs. oscillatory frequency at differing V_T's and distending pressures. (*A*) P_L = 6 cm H_2O; (*B*) P_L = 10 cm H_2O; (*C*) P_L = 25 cm H_2O; l, liter.

airway opening (Figs. 4 and 5) and corresponded closely to the classical linear inertance-resistance-compliance impedance model of lung mechanics, both qualitatively and, to a lesser degree, quantitatively. In a truly linear system, all transfer functions, including $P_{ao}/\dot{V}_{ao}$, $P_A/\dot{V}_{ao}$, and I_{ab}, must be invariant with changes in V_T. A change of these quantities, even one as large as twofold as V_T spans 16-fold, we regard as weakly nonlinear behavior. It is also noteworthy that $P_A/\dot{V}_{ao}$ and I_{ab} were systematically V_T dependent down to and including the smallest V_T's studied (5 ml), and thus no linear threshold was evident (see Figs. 5 and 8).

To interpret the tidal volume dependence of $P_A/\dot{V}_{ao}$, it is useful to consider the relationship of $\dot{V}_{ao}$ to flow through lung tissues. We could not ascertain directly what fraction of $\dot{V}_{ao}$ was shunted by central airway wall compliance, but we argue on two grounds that this fraction must have been small. First, this effect is known to be small, except when peripheral resistances are substantially elevated; because our excised lung preparation ought to correspond to the relatively bronchodilated state, no appreciable shunt would be predicted (26). Second, the alveolar pressure data of Fig. 5 represent very nearly $1/f$ frequency dependence, whereas the presence of an appreciable central shunt ought to reflect a factor of $1/f$ due to the effect of the shunt in reducing the flow delivered to the periphery, and yet another factor of $1/f$ representing the alveolar pressure response of the peripheral compliance to that flow, for an overall dependence of $1/f^2$. Thus, the data are inconsistent with the existence of an appreciable shunting of oscillatory gas flow through central airway wall compliance.

Therefore, flow through lung tissues can be approximated by $\dot{V}_{ao}$, and, thereby, the residual nonlinear effects depicted in Fig. 5 may be attributed largely to the physics of lung tissue deformation. Hildebrandt (27, 28) observed similar V_T- and f-dependent changes of lung compliance in rabbits oscillated at frequencies up to 20 Hz. He interpreted this behavior as a manifestation of plastoelastic deformation of lung tissues, in which both Newtonian and Coulomb friction combine with tissue elasticity to produce pressure-volume hysteresis that is amplitude dependent.

Alveolar pressure ratio. Earlier studies done under conditions of small V_T's have shown that alveolar pressure excursions may exceed those at the airway opening near the resonant frequency (21, 22). This resonant amplification is a consequence of the alveolar space location between the lung's major inertive (airways) and compliant (tissues) components. The observed damping of pressure amplification with increasing V_T probably reflects flow rate dependence of airways resistance (Fig. 6). Nonetheless, at resonance P_A persist substantially in excess of P_{ao} even as V_T becomes appreciable, particularly at the higher values of P_L.

Regional nonhomogeneity. The mechanical behavior of lung tissue is reasonably described as an elastic element to frequencies as high as 60 Hz (21), which is consistent with the behavior observed in these studies (Fig. 5). This implies that regional lung volume is determined by regional lung recoil, or simply P_A in the case of the excised preparation. Therefore, for fixed values of P_L, f, and V_T, the peak-to-peak P_A of the lung apex relative to that of the base can be offered as a crude

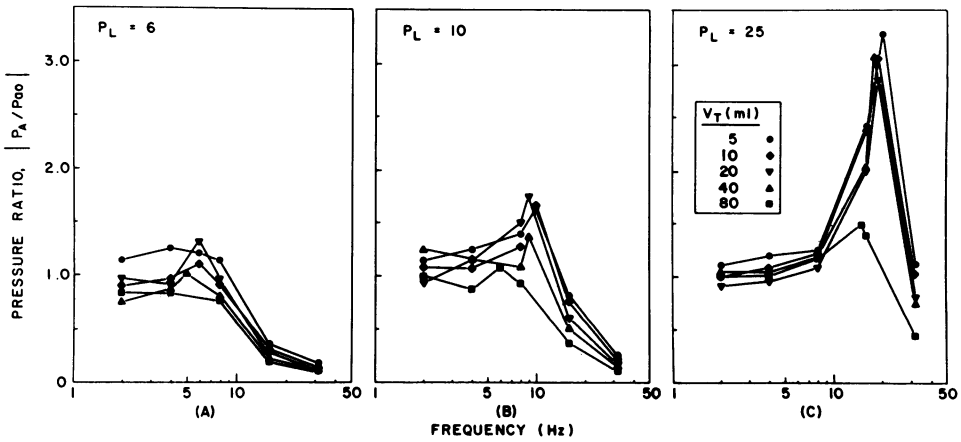

Figure 6. Alveolar pressure excursions per unit pressure at the airway opening vs. oscillatory frequency at differing V_T's and distending pressures. (*A*) P_L = 6 cm H_2O; (*B*) P_L = 10 cm H_2O; (*C*) P_L = 25 cm H_2O.

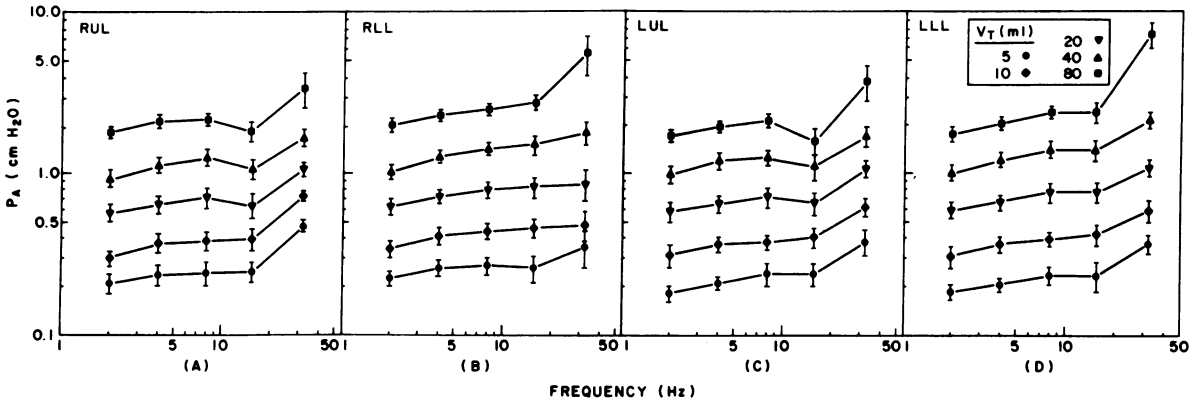

Figure 7. Alveolar pressure excursions (P_A)±SEM at different tidal volumes as measured at the four alveolar capsules vs. oscillatory frequency. P_L = 6 cm H_2O; (*A*) RUL, right upper lobe; (*B*) RLL, right lower lobe; (*C*) LUL, left upper lobe; (*D*) LLL, left lower lobe.

index of the relative excursion of regional lung volumes (Fig. 8). Although diaphragmatic lobes of the excised canine lung are stiffer than those at the apex, these differences are relatively small (24, 25). Quasistatic changes in regional lung volume engender homogeneous changes in alveolar pressure because airways gas is in hydrostatic equilibrium. The quasistatic case may be regarded as the base line that incorporates whatever nonhomogeneities in regional lung volume may be dictated by nonhomogeneous lung tissue elasticity, and upon which subsequent nonhomogeneities of alveolar pressure and lung distension evolving under dynamic conditions are superposed. The nonuniformity of this base line need not be considered further for the purposes of the discussion to follow.

Interpreted in this context, the data of Fig. 8 suggest that at low frequencies the apex and base expand nearly homogeneously, with the base favored slightly. Even at the relatively low frequency of 2 Hz, these departures of I_{ab} from unity demonstrate that intrapulmonary gas is not in hydrostatic equilibrium, and that the distribution of dynamic lung distensions has departed from the elastically controlled quasistatic case, particularly at lower values of P_L.[2] At higher frequencies, the apex receives a disproportionately larger share of V_T when V_T's are small, whereas the base receives a disproportionately larger share when V_T's are large. These mechanical data complement reports of regional nonhomogeneity of inert gas washout in the canine lung in situ (18–20), but the relationship between regional lung expansion and regional gas exchange during high frequency ventilation is unknown.

Preferential axial flow. By what mechanisms does V_T effect changes in regional lung distension? We put forward the conjecture that the geometry of central airway branching plays an important role in which there is a preference for inspired gases to follow relatively straight pathways under circumstances to be described. We call this the preferential axial flow conjecture. In the dog, the preference of the gas stream to travel with least change in direction would tend to favor filling of the base at the expense of the apex, all other factors being equal (29). The physical basis of these observations and this conjecture is elucidated by consideration of the pressures acting upon the inspired gas. The predominant mechanical pressures that might influence the distribution of inspired V_T include the following: elastic pressures distending lung tissues; unsteady inertial pressures engendered by the temporal acceleration of airways gas over the course of a cycle (P_{ua}); dynamic pressure associated with the convective momentum of gas issuing through the airways (P_{cm}); and frictional pressure losses.

Elastic pressures required to distend lung tissues are given by

$$P_{el} = V_T/C_L, \tag{1}$$

where C_L is lung compliance.

P_{ua} required for temporal acceleration are largest within the central airways (30) and are given by

$$P_{ua} = \rho(du/dt)l, \tag{2}$$

where ρ is fluid density, u is particle velocity, and l is a length representative of axial extent of the central airways. For oscillatory flows, particle velocity is related simply to V_T, cross-sectional area, and f; and time differentiation is equivalent to multiplication by $2\pi f$, so the amplitude of unsteady inertial pressure differences across the airways is approximated by

$$P_{ua} \sim 4\rho l\pi^2 f^2 V_T/A, \tag{3}$$

where A represents a cross-sectional area that typifies the central airways.

The dynamic pressure, ρu^2, can be thought of as the momentum of the fluid stream per unit area, ρu, times the rate at which that momentum is transported, u. Therefore, ρu^2 represents convective flux of fluid momentum per unit area at any given level of the airways (P_{cm}). It is important to recognize that to deflect the direction of a fluid stream through an angle θ, some other influence must provide a pressure difference proportional to $\rho u^2 \sin\theta$ to balance the change in vector momentum. Such influences include unsteady inertia, friction, and tissue elasticity in each of the daughter airways. Given no such influence, or inadequate ones, the tendency of the fluid stream is to continue with least direction change. Convective momentum flux, like unsteady inertia, is expected to be greatest in the central airways, where fluid velocities are largest and may be expressed as

2. At frequencies well below resonance, where inertial effects are negligible, I_{ab} is readily calculated for the case of a two compartment model with different resistance-compliance time constants,

$$I_{ab} = \frac{P_A}{P_B} = \left[\frac{1 + (2\pi f R_B C_B)^2}{1 + (2\pi f R_A C_A)^2}\right]^{1/2}, \quad f \ll f_0.$$

Thus, I_{ab} being less than unity at low frequencies implies that the time constant of the base is smaller than that of the apex.

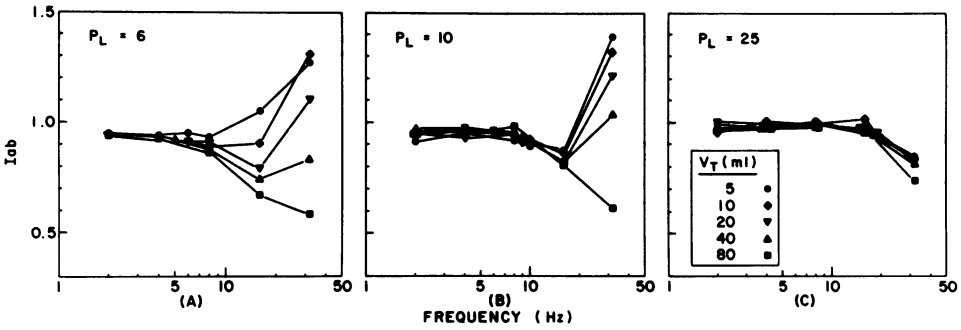

Figure 8. Ratio of alveolar pressure excursions at the apex to those at the base, which is taken to be an index of relative lung distension vs. oscillatory frequency at differing V_T's and distending pressures. (*A*) P_L = 6 cm H_2O; (*B*) P_L = 10 cm H_2O; (*C*) P_L = 25 cm H_2O.

$$P_{cm} \sim \rho(f V_T/A)^2. \quad (4)$$

Frictional pressure losses will be considered later.

Using these expressions, the relative importance of P_{ua} and P_{el} is approximated by

$$P_{ua}/P_{el} \sim 4\pi^2 f^2(\rho l/A)C \sim (f/f_0)^2, \quad (5)$$

where $\rho l/A$ is identified as airway inertance and f_0 is lung resonant frequency. This result is the familiar one showing that elastic pressures dominate when oscillatory frequency is much smaller than resonant frequency, whereas unsteady inertial pressures are much larger than elastic pressures when oscillatory frequency exceeds resonant frequency. Note that the expression is independent of V_T, but is influenced by P_L insofar as C_L and to a lesser degree l and A might vary with the degree of lung inflation and thereby alter lung resonant frequency. Resonant frequency can be determined empirically from the impedance minima of Fig. 4, or the resonant peak of the pressure ratio (Fig. 6).

The importance of P_{cm} relative to P_{ua} is approximated by combining Eqs. 3 and 4,

$$P_{cm}/P_{ua} \sim V_T/(lA) \sim V_T/V_D^*, \quad (6)$$

where V_D^* has the dimensions of volume and is the product of A, a cross-sectional area typical of the central airways, and l, a length scale typical of their axial extent.[3] We assert without elaboration that this volume, V_D^*, is proportional to and somewhat less than anatomic dead space, and ought not include the volume of the common pathway mouthward of the carina, regarding which questions of distribution are moot. Because of the crude nature of this analysis, values on the order of 2 ml/kg seem to be appropriate for V_D^*, corresponding to absolute volumes of 20 ml for the dogs used in this study. Typical anatomic dead space would be closer to 40 ml.

It is noteworthy that the relative importance of unsteady inertia and convective inertia during oscillatory forcing is independent of oscillatory frequency, and also independent of gas density. Classically, the relative importance of these quantities (Eq. 6) is the reciprocal of the Strouhal number. It is worthwhile to note, therefore, that frequency sweeps of constant V_T represent iso-Strouhal contours, in which the relative importance of unsteady inertia and convective inertia is fixed (Fig. 8). For the most part, the data of Fig. 8 may be interpreted quite simply in light of these two nondimensional quantities, f/f_0 and V_T/V_D^*. Consider the following limiting situations.

First, at very small frequencies ($f/f_0 \ll 1$) elastic pressures dominate both manifestations of fluid inertia, unsteady and convective. The elastically controlled plateau persists to higher frequencies at larger P_L's, corresponding to the observed increase in f_0 with P_L (Fig. 8).

Second, in the case where frequency is high ($f/f_0 \gg 1$) and V_T is small ($V_T/V_D^* \ll 1$) unsteady fluid inertia is expected to be the dominant mechanical effect. Thereby, we interpret the preference of apical distension at the expense of the base ($I_{ab} > 1$) to indicate that the airway inertance of pathways leading to the lobes of the apex is less than that of pathways to the base. Because airways inertance is $\rho l/A$, these data imply larger diameter bronchi and/or shorter pathways for airways serving the apex compared with those of the base. From the morphometric canine data of Woldehivot and Horsfield (29), we computed the inertance of selected bronchial pathways (Fig. 9) and predicted the relative flows to the associated pathways for the limiting circumstance in which flow distribution is controlled by unsteady fluid inertia. Thus, one would expect

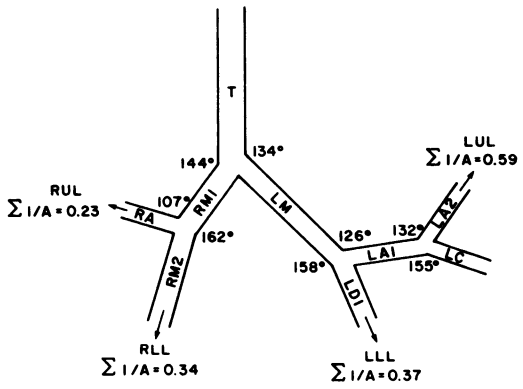

Figure 9. Relative inertance and branching angles of four selected pathways in the canine lung (from the morphometric data of Woldehivot and Horsfield [29]). Only the most central airways are diagrammed. RUL, RLL, LUL, and LLL indicate right upper and lower and left upper and lower lobes, respectively. $\Sigma\ l/A$ represents length (mm) divided by area (mm^2) for each path segment, summed over all the path segments in a given pathway. $\Sigma\ l/A$ is thus an index of the inertance of any given path (see text). LA1, left common apical bronchus; LA2, left apical lobe branch; LC, cardiac lobe branch; LD1, left diaphragmatic bronchus; LM, left main bronchus; RA, right apical lobe bronchus; RM1, right main bronchus; RM2, continuation of RM1; T, trachea.

3. The ratio of convective momentum to unsteady inertia, given by V_T/V_D^*, may also be expressed as Re/alpha^2, i.e., the Reynolds number (convection/friction) divided by the square of the Womersley parameter (unsteady inertia/friction).

right upper lobe flow to exceed left upper lobe flow under these circumstances, while flow to the right and left lower lobes would be expected to be about the same. Furthermore, flow to the apex is expected to exceed that to the base. These conditions are most closely approximated in our experiments at the highest frequency (32 Hz) and lowest V_T (5 ml). Recognizing that there may have been anatomical differences between our dogs and those of Woldhivot and Horsfield (29), and that a distribution of flow controlled solely by unsteady fluid inertia may not have been achieved by 32 Hz, comparison between our observations and morphometric predictions reveals reasonable correspondence (Fig. 7). Thus, considering the entire range of frequencies, when V_T's are very small, $V_T/V_D^* \ll 1$, the distribution of inspired gas is well characterized by linear mechanical phenomena because in that circumstance both lung elasticity and fluid inertia would be well approximated by linear processes. In this case impedance models are valid and the angle of airway bifurcations is of little consequence (31).

Third, in the case in which f is above resonance ($f/f_0 \gg 1$) and V_T is large ($V_T/V_D^* \gg 1$), tissue elastic and unsteady inertial pressures are small compared with the convective momentum flux, and thereby, would be incapable of redirecting the vector momentum of the inspiratory gas stream.[4] As a result, the inspiratory gases would tend to flow along the straightest airway path at any given bifurcation, with changes in direction along the preferred paths effected by the pressure distribution on the airway walls. This phenomenon, which we call preferential axial flow, is an intrinsically nonlinear phenomenon and is hypothesized to control the distribution of inspired V_T when f and V_T are large. The morphometric data of Woldhivot and Horsfield (29) concerning branching angles of the major airways of the dog reveal that on both the right and the left side, the straightest pathways are directed towards the base, while turns through more acute angles are encountered along the pathways to the apex (Fig. 9). Thus, we would expect that flow to the base would be favored over flow to the apex under these conditions. Fig. 8 shows that this was the case.

Also, in the case of steady inspiratory flow through an airway cast, both elastic and unsteady inertial pressure differences vanish, and so, accordingly, convective momentum flux would control the distribution of flow when Reynolds numbers are large. As is consistent with the data of Fig. 8, preferential flow to the basilar regions has been reported in such circumstances (7–9). Snyder and colleagues (7, 8) have attributed this phenomenon to skewing of the inspiratory axial velocity profile upstream of the bifurcation. While such nonuniformities of the axial velocity profile could undoubtedly influence the distribution of flow at the bifurcation, we suspect that they need not be postulated to account for preferential axial flow at an asymmetrical bifurcation. To the extent that the explanations offered above are correct, the total momentum flux of the fluid stream and the geometry of the bifurcation would be seen as the primary influences, whereas nonuniformities of the axial momentum profile across the stream would be seen as a correction that could appreciably alter flow distribution only in the cases of symmetrical branching geometries or unusual velocity profiles.

4. Having achieved a distribution dependent on convective momentum flux, it is possible that the Coanda effect might further stabilize this distribution.

The following intermediate cases are of interest. When $f/f_0 \gg 1$, but $V_T/V_D^* \sim 1$, elastic pressures are negligible, unsteady inertia and convective momentum flux are of comparable magnitude, and the distribution of inspired gas is relatively homogeneous. When $f/f_0 \sim 1$, elastic pressures and unsteady inertial pressures are of equal importance, opposite in sign, and so cancel each other out. This cancellation might provide a window through which convective momentum flux could dominate even when $V_T/V_D^* < 1$, or, depending upon Reynolds number, frictional pressure losses might control the distribution of inspired gases. These might be reflected by the biphasic regional distribution observed in most of the tidal volume sweeps (Fig. 8).

To what degree might frictional losses play a role? In the case where $V_T/V_D^* \ll 1$ linear oscillation mechanics prevail. Frictional pressure losses, if they are important at all in controlling regional distributions, would be most important in the vicinity of the resonant frequency, where elastic and unsteady inertial pressures cancel. At higher frequencies, frictional pressure losses are expected to become decreasingly significant in relation to unsteady inertia. However, the regional nonhomogeneity was observed to increase at higher frequencies (Fig. 8), and thus frictional pressure losses could not be responsible for the increase in I_{ab} with frequency when V_T/V_D^* is small. On the other hand, when V_T/V_D^* is large, the relative importance of fluid momentum to friction is, by definition, the Reynolds number, which varied in the trachea from 500 to 50,000 in our studies ($Re = Ud/\gamma = 4fV_T/d\gamma$ [in which U is velocity, d is diameter, and γ is kinematic viscosity]). Reynolds number increases with frequency for fixed V_T, and therefore frictional pressures would be expected to have a diminishing role relative to convective momentum as frequency is increased, and could not account for the progressive departure of I_{ab} from unity with frequency when V_T/V_D^* is large. With regard to the high Reynolds number case, Slutsky et al. (9) found that the distribution of steady inspiratory flow in an airway cast increasingly favored the lower lobar bronchi as tracheal Reynolds number increased, and suggested that this arose because the frictional pressure losses introduced by branching might increase with both flow rate and branching angle. While we do not believe that there are sufficient data to decide whether this flow nonhomogeneity reflects the influence of convective momentum rather than frictional pressure differences, we favor the former idea. Finally, with regard to the case when Reynolds numbers are small compared with unity, convective momentum could not appreciably influence the distribution of flow.

Dynamic hyperinflation of the lung during high frequency oscillations may influence the interpretations offered above. Simon et al. (32) have shown that mean (time averaged) alveolar pressure exceeds that at the airway opening during high frequency oscillations. Furthermore, we have reported that this dynamic hyperinflation phenomenon is nonuniform in the excised canine lung, with mean alveolar pressure at the base exceeding that at the apex by up to 3 cm H_2O at high f and V_T (33). This could result in the lower lobes lying on a substantially stiffer part of their local pressure-volume curve, and an I_{ab} of <1.0 even if apical and basal volume excursions were identical. Thus, the apex-to-base ratio of regional pressure excursions, I_{ab}, might underestimate the apex-to-base ratio of regional volume excursions under circumstances of high f and V_T. However, we used the regional mean alveolar pressure

data of Allen et al. (33) as a guide to estimate the resulting regional compliance changes based on the average pressure-volume curves of these six excised lungs and found that these changes alone could not account for the observed changes in I_{ab}, although they may contribute.

Implications for HFV. These data suggest that to a crude approximation the pressure costs required to drive gas into nonbronchoconstricted lung during HFV can be described usefully by a simple inertance-resistance-compliance impedance model. The major departure of lung behavior from this model is plastoelastic deformations of lung tissues, which causes effective lung compliance to increase with increasing V_T. As we have demonstrated previously, near resonance pressure excursions in the alveolar compartments can substantially exceed those at the airway opening (21, 22). The degree of amplification of alveolar pressure diminishes as V_T increases, but is still substantial as V_T's approach or exceed those used during HFV. Our data also demonstrate that at the resonant frequency, pressure excursions per unit flow in central airways is the least (Fig. 4), while pressure excursions in peripheral airways per unit flow fall monotonically as frequency increases (Fig. 5). Thus, both low V_T data (21, 22) and the present study imply on mechanical grounds that to minimize pressure swings in central airways, one might choose to ventilate at the resonant frequency, but that above resonance, pressure excursions in small airways might be decreased at the expense of increased pressure excursions centrally.

The relationship of regional lung expansion (Fig. 8) to regional gas exchange during HFV is unclear. An early theoretical study (34) predicted and later experimental studies (35–38) confirmed that overall gas exchange during HFV would depend upon the product of f and V_T, rather than each individually, in the limit when V_T's were infinitesimally small compared with dead space, and that there would be an independent influence of V_T upon gas exchange when V_T's approached appreciable fractions of the dead space, i.e., when bulk convection would become significant relative to gas mixing phenomena. It has also been speculated that the independent V_T effect might be due to direct ventilation of nearby alveoli in the asymmetrical airway tree (39), due to complexities in characterizing the gas concentration boundary conditions at the airway opening and at the alveolus (36, 40), due to streaming flows (41), and due to the physics of compartmental mixing (42).

The data of Fig. 8 suggest yet another independent influence of V_T upon gas exchange, namely alterations of the regional distribution of lung distension and, inferentially, the distribution of ventilation. Conversely, it has not escaped our attention that apical or diaphragmatic lung regions might be ventilated preferentially by judicious selection of f, V_T, and P_L in a manner that alters the match of ventilation to perfusion. While these studies included neither the chest wall nor gradients in pleural pressure, the similarity of the mechanical nonhomogeneities described above to inert gas washout nonhomogeneities in situ reported in dogs (18, 19) and humans (43) implies the relevance of the mechanical factors described above to the intact subject. In studies of regional ^{133}Xe clearance rates during HFV, Rehder and Didier (43) noted that in humans, apical nondependent regions exhibit faster clearance of ^{133}Xe, while in dogs (20) basilar nondependent regions clear faster. Venegas et al. (18) and Brusasco et al. (19) also found preferential basilar clearing at high V_T. These differences in regional clearance patterns might be related in part to differences in V_T/V_D* ratios used in those studies, as the animals were ventilated with stroke volumes ranging from 2.6 to 3.7 ml/kg, while the stroke volume used in the human study was 1.1 ml/kg.

More general implications. These studies complement and extend many earlier studies of the distribution of ventilation under more physiological conditions, in which the importance of the distribution of elasticity, friction, and to some degree, inertia, have been identified, along with non-uniformity of driving pressure. Our present study focuses largely on the influences of fluid inertia upon the distribution of ventilation, and demonstrates that fluid inertia may be manifested in two ways, unsteady acceleration and convective momentum flux. This idea adds some insights to the results of Bake et al. (12), in which the effect of increasing inspiratory flow rate upon the distribution of ventilation was shown to favor the lung apex. However, careful examination of their data reveals that after the initial increment of flow, in only three of seven subjects did further increases of flow rate increasingly favor the apex, while in three of the seven the opposite tendency was true. Such an outcome is consistent with the influence of convective momentum flux associated preferential axial flow, as elaborated above. The importance of this effect compared with non-uniformity of pleural pressure (44) is unclear at this time.

Finally, our data and the influence of convective inertia in influencing the distribution of flow may be related to the nature of aerodynamic valving in avian lungs as first described by Hazelhoff (45). To the degree that such valving works based upon the principle that convective inertia promotes preferential axial flow, the unidirectional function of such valves might be expected to fail when convective inertia becomes small with respect to unsteady inertial, elastic, or frictional pressures.

Acknowledgments

We wish to thank Svetlana Gitin for her assistance in reducing and plotting the data, and Richard Close for his assistance in animal preparation and surgery.

This research was supported in part by the Puritan-Bennett Foundation, and National Heart, Lung, and Blood Institute grants HL26800, HL29706, HL33009, and HL27372.

References

1. Otis, A. B., C. B. McKerrow, R. A. Bartlett, J. Mead, M. B. McIlroy, N. J. Silverstone, and E. P. Radford, Jr. 1956. Mechanical factors in distribution of pulmonary ventilation. *J. Appl. Physiol.* 8: 427–443.

2. Milic-Emili, J., J. A. M. Henderson, M. B. Dolovich, D. Trop, and K. Kaneko. 1966. Regional distribution of inspired gas in the lung. *J. Appl. Physiol.* 21:749–759.

3. Dollfuss, R. E., J. Milic-Emili, and D. V. Bates. 1967. Regional ventilation of the lung, studied with boli of 133 xenon. *Respir. Physiol.* 2:234–246.

4. Fredberg, J. J., and J. Mead. 1979. Impedance of intrathoracic airway models during low frequency periodic flow. *J. Appl. Physiol. Respir. Environ. Exercise Physiol.* 47:347–351.

5. Slutsky, A. S., G. G. Berdine, and J. M. Drazen. 1981. Oscillatory flow and quasi-steady behavior in a model of human central airways. *J. Appl. Physiol. Respir. Environ. Exercise Physiol.* 50:1293–1299.

6. Michaelson, E. D., E. D. Grassman, and W. R. Peters. 1975.

Pulmonary mechanics by spectral analysis of forced random noise. *J. Clin. Invest.* 56:12190–1230.

7. Snyder, B., D. R. Dantzker, and M. J. Jaeger. 1981. Flow partitioning in symmetric cascades of branches. *J. Appl. Physiol. Respir. Environ. Exercise Physiol.* 51:598–606.

8. Snyder, B., and M. J. Yeager. 1983. Lobar flow patterns in a hollow cast of canine central airways. *J. Appl. Physiol. Respir. Environ. Exercise Physiol.* 54:749–756.

9. Slutsky, A. S., G. G. Berdine, J. M. Drazen. 1980. Steady flow in a model of human central airways. *J. Appl. Physiol. Respir. Environ. Exercise Physiol.* 49:417–423.

10. Isabey, D. 1982. Steady and pulsatile flow distribution in a multiple branching network with physiological applications. *J. Biomech.* 15:395–404.

11. Chang, H. K., and O. A. El Masry. 1982. A model study of flow dynamics in human central airways. I. Axial velocity profiles. *Respir. Physiol.* 49:75–95.

12. Bake, B., L. Wood, B. Murphy, P. T. Macklem, and J. Milic-Emili. 1974. Effect of inspiratory flow rate on regional distribution of inspired gas. *J. Appl. Physiol.* 37:8–17.

13. Forkert, L., N. R. Anthonisen, and L. D. H. Wood. 1978. Frequency dependence of regional lung washout. *J. Appl. Physiol. Respir. Environ. Exercise Physiol.* 45:161–170.

14. Kronenberg, R. S., O. D. Wangensteen, and R. A. Pouto. 1976. Frequency dependence of regional lung clearance of 133XE in normal man. *Respir. Physiol.* 27:293–303.

15. Robertson, P. C., N. R. Anthonisen, and D. Ross. 1969. Effect of inspiratory flow rate on regional distribution of inspired gas. *J. Appl. Physiol.* 26:438–443.

16. Pedley, T. J., M. F. Swallow, and J. Milic-Emili. 1972. A non-linear theory of distribution of pulmonary ventilation. *Respir. Physiol.* 15:1–38.

17. Shykoff, B. E., A. van Grondelle, and H. K. Chang. 1982. Effects of unequal pressure swings and different waveforms on distribution of ventilation: a non-linear model simulation. *Respir. Physiol.* 48:157–168.

18. Venegas, J. G. 1983. Efficiency and distribution of high frequency ventilation. PhD Thesis. Massachusetts Institute of Technology.

19. Brusasco, V., T. J. Knopp, and K. Rehder. 1983. Gas transport during high frequency ventilation. *J. Appl. Physiol. Respir. Environ. Exercise Physiol.* 55:472–478.

20. Schmid, E. R., T. J. Knopp, and K. Rehder. 1981. Intrapulmonary gas transport and perfusion during high frequency oscillation. *J. Appl. Physiol. Respir. Environ. Exercise Physiol.* 51:1507–1514.

21. Fredberg, J. J., D. H. Keefe, G. M. Glass, R. G. Castile, and I. D. Frantz III. 1984. Alveolar pressure nonhomogeneity during small amplitude high frequency oscillation. *J. Appl. Physiol. Respir. Environ. Exercise Physiol.* 57:788–800.

22. Allen, J. L., J. J. Fredberg, D. H. Keefe, G. M. Glass, and I. D. Frantz III. 1985. Alveolar pressure magnitude and asynchrony during high frequency oscillation. *Am. Rev. Resp. Dis.* In press.

23. Brusasco, V., K. Rehder, K. C. Beck, and M. Crawford. 1985. Gas volume delivered by high frequency ventilation. *Fed. Proc.* 44: 1383. (Abstr.)

24. Faridy, E. E., R. Kidd, and J. Milic-Emili. 1967. Topographical distribution of inspired gas in excised lobes of dogs. *J. Appl. Physiol.* 22(4):760–766.

25. Frank, N. R. 1963. A comparison of static volume-pressure relations of excised pulmonary lobes of dogs. *J. Appl. Physiol.* 18:274–278.

26. Mead, J. 1969. Contribution of compliance of airways to frequency-dependent behaviour of lungs. *J. Appl. Physiol.* 26:670–673.

27. Hildebrandt, J. 1969. Comparison of mathematical models for cat lung and viscoelastic balloon derived by Laplace transform methods from pressure-volume data. *Bull. Math Biophys.* 31:651–667.

28. Hildebrandt, J. 1970. Pressure-volume data of cat lung interpreted by a plastoelastic, linear viscoelastic model. *J. Appl. Physiol.* 28(3):365–372.

29. Woldehivot, Z., and K. Horsfield. 1978. Diameter, length, and branching angles of the upper airways in the dog lung. *Respir. Physiol.* 33:213–218.

30. Mead, J. 1956. Measurement of inertia of the lungs at increased ambient pressure. *J. Appl. Physiol.* 9:208–212.

31. Strutt, J. W. (Baron Rayleigh). 1945. The Theory of Sound. Vol. II. Dover, New York. 62.

32. Simon, B. A., G. G. Weinmann, and W. Mitzner. 1984. Mean airway pressure and alveolar pressure during high frequency ventilation. *J. Appl. Physiol. Respir. Environ. Exercise Physiol.* 57:1069–1078.

33. Allen, J., I. Frantz III, and J. Fredberg. 1984. Mean alveolar pressures during high frequency oscillations. *Physiologist.* 27:212. (Abstr.)

34. Fredberg, J. J. 1980. Augmented diffusion in the airways can support pulmonary gas exchange. *J. Appl. Physiol. Respir. Environ. Exercise Physiol.* 49:232–238.

35. Slutsky, A. S., J. M. Drazen, R. H. Ingram, Jr., R. D. Kamm, A. H. Shapiro, J. J. Fredberg, S. H. Loring, and J. Lehr. 1980. Effective pulmonary ventilation with small-volume oscillations at high frequency. *Science (Wash. DC).* 209:609–611.

36. Slutsky, A. S., R. D. Kamm, T. H. Rossing, S. H. Loring, J. Lehr, A. H. Shapiro, R. H. Ingram, Jr., and J. M. Drazen. 1981. CO_2 elimination in dogs by high frequency (3–30 Hz), low tidal volume ventilation: effects of frequency, tidal volume and lung volume. *J. Clin. Invest.* 68:1475–1484.

37. Ngeow, Y. K., and W. Mitzner. 1982. A new system for ventilating with high-frequency oscillation. *J. Appl. Physiol. Respir. Environ. Exercise Physiol.* 53:1638–1642.

38. Zidulka, A., D. Gross, H. Minami, V. Vartion, and H. K. Chang. 1983. Ventilation by high frequency chest wall compression in dogs with normal lungs. *Am. Rev. Respir. Dis.* 127:709–713.

39. Chang, H. K. 1984. Mechanism of gas transport during ventilation by high frequency oscillations. *J. Appl. Physiol. Respir. Environ. Exercise Physiol.* 56:553–563.

40. Khoo, M. C. K., A. S. Slutsky, J. M. Drazen, J. Solway, N. Gavriely, and R. D. Kamm. 1982. An improved model of gas transport during HFV. *Physiologist.* 25:283. (Abstr.)

41. Haselton, F. R., and P. W. Scherer. 1980. Bronchial bifurcations and respiratory mass transport. *Science (Wash. DC).* 208:69–71.

42. Weinmann, G. G., W. Mitzner, and S. Permutt. 1984. Physiologic dead space during high frequency ventilation in dogs. *J. Appl. Physiol. Respir. Environ. Exercise Physiol.* 57:881–887.

43. Rehder, K., and E. P. Didier. 1984. Gas transport and pulmonary perfusion during high frequency ventilation in humans. *J. Appl. Physiol. Respir. Environ. Exercise Physiol.* 57:1231–1237.

44. Fixley, M. S., C. S. Roussos, B. Murphy, R. R. Martin, and L. A. Engel. 1978. Flow dependence of gas distribution and the pattern of inspiratory muscle contraction. *J. Appl. Physiol. Respir. Environ. Exercise Physiol.* 45:733–741.

45. Hazelhoff, E. H. 1951. Structure and function of the lung of birds. *Poult. Sci.* (Suppl. 1):3–10.